The Stiffness of Tensegrity Structures

S.D. Guest
Department of Engineering, University of Cambridge,
Trumpington Street, Cambridge CB2 1PZ, UK

March 23, 2010

Abstract

The stiffness of tensegrity structures comes from two sources: the change of force carried by members as their length is changed, and the reorientation of forces as already stressed members are rotated. For any particular tensegrity, both sources of stiffness may have a critical role to play. This paper explores how the stiffness of two example tensegrity structures changes as the level of prestress in a member varies. It is shown that, for high levels of prestress, an originally stable tensegrity can be made to have zero stiffness, or indeed be made unstable.

1 Introduction

Tensegrities form remarkable structures. They are frequently visually arresting (Heartney, 2009); and they can be designed to give 'optimal' structures Masic et al. (2006). The present paper will discuss the stiffness of tensegrity structures — the first order change of force carried as the structures is deformed. There are two competing sources for a tensegrity's stiffness, and the balance between these sources changes as the prestress varies. Thus, for instance, the paper will show that, for a 'stable' tensegrity, increasing a low level of prestress will increase the stiffness; however, for a high level of prestress, a further increase in prestress may reduce the stiffness, and even lead to a structure with zero or negative stiffness.

The definition of 'tensegrity' is a subject of debate (see, e.g., Motro, 2003). At one extreme is the mathematical definition (Roth and Whiteley, 1981; Connelly and Whiteley, 1996) that a tensegrity is a structure consisting of 'cables' (members only able to resist tension), 'struts' (members only able to resist compression, e.g. a contact force) and 'bars' (members able to resist tension and compression. Others might insist that a tensegrity must have compression members that do not touch, or must have an infinitesimal mechanism. The present paper will not enter the debate on definition, except to note that the basic formulation used here is valid for any prestressed

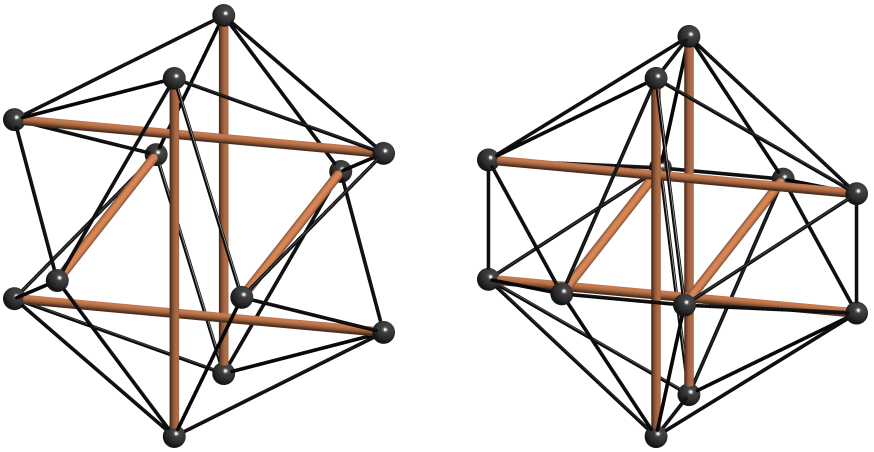

Tensegrity A
(a)

Tensegrity B
(b)

Figure 1: Two tensegrities used as examples. Tensegrity A is the classic 'expanded octahedron' tensegrity, which has one state of self-stress and one infinitesimal mechanism. Tensegrity B has the same arrangement of struts and cables as Tensegrity A, but with additional cable pulling pairs of nodes closer together; Tensegrity B does not have an infinitesimal mechanism.

structure, and that at least one of the tensegrities used as examples satisfies even the most stringent definition of tensegrity.

By way of example, the paper will show results for the two tensegrity structures shown in Figure 1. Tensegrity A is the classic example described by Pugh (1976) as the 'expanded octahedron' tensegrity. It consists of $j = 12$ nodes, and $b = 30$ members, made up of 24 cables and 6 struts. Using an extended Maxwell rule (Calladine, 1978) relating the number of infinitesimal mechanisms m and states of self-stress s gives

$$m - s = 3j - b - 6 = 0. \tag{1}$$

Tensegrity A has T_h symmetry (in the Schoenflies notation, see e.g. Altmann and Herzig, 1994), with symmetry elements that consist of four three-fold axes, three two-fold axes, and three planes of reflection. Symmetry defines the position of all nodes in terms of one reference node, shown in Figure 2: for Tensegrity A to be prestressed ($s \neq 0$) the parameter p must take the value 0.5, which can be confirmed by simple statics, or the use of matrix methods, as described by Pellegrino and Calladine (1986) and Pellegrino (1993). The presence of a state of self-stress guarantees, from (1), the existence of an infinitesimal mechanism (for this mode, to first order, nodal movement results in zero extension of every member).

Tensegrity B is a variation on Tensegrity A, designed to not have an

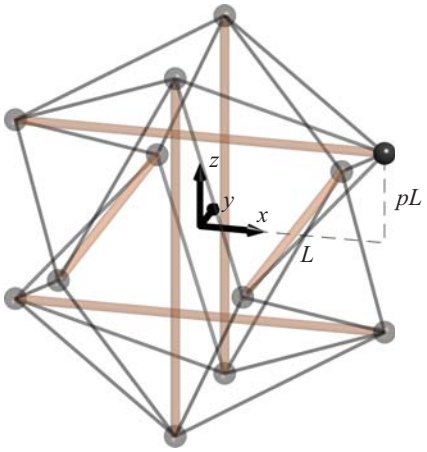

Reference node position

$$\mathbf{p}_r = \begin{bmatrix} 1 \\ 0 \\ p \end{bmatrix} L$$

Figure 2: The coordinates of a single node for both tensegrity A when $p = 1/2$, and tensegrity B when $p = 1/3$. For comparison, the vertices of a regular icosahedron have $p = 2/(1 + \sqrt{5}) = 0.618$.

infinitesimal mechanism. Six cables have been added between nodes so that the cable net forms the edges of an (irregular) icosahedron. Thus the structure consists of $j = 12$ nodes, and $b = 36$ members, made up of 30 cables and 6 struts, and the extended Maxwell rule gives

$$m - s = 3j - b - 6 = -6. \tag{2}$$

In fact, $m = 0$ is guaranteed in this case as the cable-net alone forms the edges of a convex triangulated polyhedra (Cauchy, 1813; Dehn, 1916), and the addition of six internal struts can only add to the states of self-stress to give $s = 6$. For tensegrity B, the value $p = 1/3$ is chosen, as in this case, the totally symmetric state of self-stress (which could be found by, e.g., the methods described by Kangwai and Guest, 2000) has equal tension coefficients (tension/length) in all cables.

Both Tensegrity A and Tensegrity B are 'super-stable', in the notation of Connelly (1999). This means that prestress properties could not be more benign — but despite this, it will be shown in Section 6 that both structures can be made unstable for sufficiently high levels of prestress.

In this paper, for both Tensegrity A and Tensegrity B, it will be assumed that the struts are axially rigid, but the cables are axially flexible. For each tensegrity, two contrasting material properties for the cables will be considered. Firstly, a set of stiff cables will be considered, for which a typical graph of tension against length is shown in Figure 3(a). A key dimensionless parameter in the stiffness formulation used in this paper, as described in Section 2, is the ratio of the tension coefficient, $\hat{t} = t/l$ to the

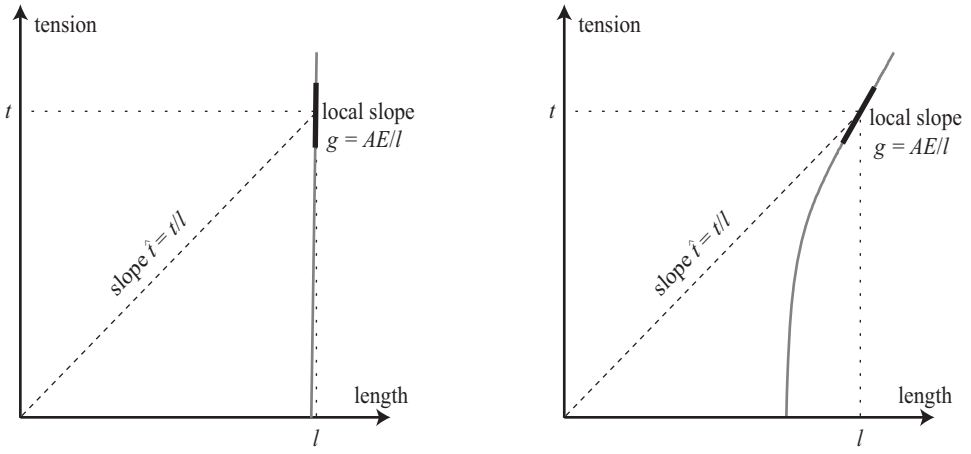

Figure 3: Material properties for two contrasting sets of cables. In (a) the cables are stiff, made of, for instance, steel, and $t/l \ll dt/dl$. In (b), the cables are assumed to be compliant, made of, in this instance, an elastomer where $t/l \not\ll dt/dl$. Note that, for a cable with the same cross-sectional area, the values of force in (a) are likely to be very much higher than those in (b), as the Young's Modulus of a steel will be the order of a hundred times stiffer than the Young's Modulus of an elastomer.

axial stiffness $g = dt/dl$,

$$\varepsilon = \frac{t/l}{dt/dl}. \tag{3}$$

Locally to the working point of the cable, we can define a Young's Modulus E for the material, and a cross-sectional area of the cable A, so that the axial rigidity is $g = AE/l$. Thus, we can define the parameter ε as a nominal strain

$$\varepsilon = \frac{t}{AE}. \tag{4}$$

For metallic cables, the slope g will be essentially linear before yield, and hence for such stiff cables, ε must be less than the yield strain, and consequently $\varepsilon \ll 1$. In Section 3 we will assume $\varepsilon = 0.01$.

A contrasting set of material properties will also be considered, when the cables are compliant, being made of e.g. rubber, or some other elastomer. For these materials, a typical graph of tension against length is shown in Figure 3(b). Now the dimensionless parameter ε is not limited to being much less than one. In Section 4 a value of 0.6 will be assumed.

2 Stiffness formulation

The basic stiffness formulation that will be used is described in Guest (2006); an identical formulation with an alternative notation is described in Skelton and de Oliveira (2009). The tangent stiffness matrix $\mathbf{K}$ relates, to first order, the displacements at each of the 12 nodes in the x-, y- and z-directions, written as a vector $\mathbf{d}$, to the applied load at each of the nodes, written as a vector $\mathbf{p}$,

$$\mathbf{K}\mathbf{d} = \mathbf{p}. \tag{5}$$

The matrix $\mathbf{K}$ depends on the configuration of the structure, the axial stiffness of the members (the slope $g = dt/dl$ shown in Figure 3) and the tension coefficient carried by the members (the slope $\hat{t} = t/l$ shown in Figure 3). It can be written as

$$\mathbf{K} = \mathbf{A}\hat{\mathbf{G}}\mathbf{A}^{\mathrm{T}} + \mathbf{S}. \tag{6}$$

In (6), $\mathbf{A}$ is the *equilibrium matrix* for the structure — a matrix of direction cosines describing the equilibrium relationship between internal forces in the members $\mathbf{t}$ and applied loads at nodes $\mathbf{p}$, $\mathbf{A}\mathbf{t} = \mathbf{p}$ (Pellegrino, 1993); $\mathbf{A}^{\mathrm{T}}$ equivalently describes the first-order kinematic relationship between the displacement of nodes $\mathbf{d}$ and the extensions of members $\mathbf{e}$. $\hat{\mathbf{G}}$ is a diagonal matrix of modified axial stiffnesses, with an entry for each member i ($1 \leq i \leq b$),

$$\hat{g}_i = g_i - \hat{t}_i, \tag{7}$$

which can be written in terms of the nominal strain for the member, ε_i, as

$$\hat{g}_i = g_i(1 - \varepsilon_i). \tag{8}$$

$\mathbf{S}$ is the (large) *stress matrix* for the structure. $\mathbf{S}$ can be written as the Kronecker product of a *small* or *reduced* stress matrix $\mathbf{\Omega}$ and a 3-dimensional identity matrix $\mathbf{I}$

$$\mathbf{S} = \mathbf{\Omega} \otimes \mathbf{I} \tag{9}$$

and the coefficients of the small stress matrix are given by

$$\Omega_{ij} = \begin{cases} -\hat{t}_{i,j} = -\hat{t}_{j,i} & \text{if } i \neq j, \text{ and \{i,j\} a member,} \\ \sum_{k \neq i} \hat{t}_{ik} & \text{if } i = j, \\ 0 & \text{if there is no connection between } i \text{ and } j. \end{cases} \tag{10}$$

In this formulation, $\hat{t}_{i,j}$ is the tension coefficient (t/l) in the member that runs between nodes i and j (there will be a unique mapping between the pair (i, j) and the bar numbering described above for $\hat{\mathbf{G}}$). It was shown in Schenk et al. (2007) that, for a self-stressed structure, the stress matrix $\mathbf{S}$ must have a nullity of at least 12 (and, it turns out, exactly 12 for both Tensegrity A and Tensegrity B), and can provide no stiffness to any of the 6

rigid body modes, or to any of the 6 *affine deformation* modes, i.e., modes in which the body is deformed uniformly by stretching or shear.

For both tensegrities A and B, the stiffness matrix $\mathbf{K}$ is a symmetric matrix of dimension 36×36. In fact, for the results reported here, a change of coordinates was used to condense out two sets of freedoms from the original 36: the 6 rigid-body modes, and the 6 modes that correspond to extension of the struts. The effect of this is to leave an 24×24 symmetric matrix, for which the eigenvalues are then found. These 24 eigenvalues have at most 10 distinct values (as can be predicted by a symmetry analysis of the original system, as described by Kangwai et al., 1999). Condensing out the six modes corresponding to extensions of struts essentially makes the assumption that the struts are rigid. An alternative procedure would have been to have given the struts a stiffness of, say, 1000 times the value of the stiffness of the cables, and worked with the original 36×36 matrix. This would have given essentially the same set of 24 eigenvalues, plus an additional 6 eigenvalues which are approximately 1000 times as large, and 6 zero eigenvalues corresponding to rigid body modes.

The complete set of eigenvalues for varying levels of prestress will be reported in Section 6, but first the paper will concentrate on just two modes, shown in Figure 4. Mode 1 corresponds to the infinitesimal mechanism for tensegrity A, and is an eigenmode of the stiffness matrix for all levels of prestress. Mode 2 is a shear mode, and is actually an eigenmode only for a prestress corresponding to a nominal strain $\varepsilon = 1$; however, for other levels of prestress results are reported for the eigenmode which is closest to this.

3 Stiff cables/low relative prestress

This section will consider the results that are appropriate for cases where the stiffness of the cables g is much greater than the current tension coefficient, t/l, for instance the case shown in Figure 3(a). This would be typical of tensegrities constructed with, e.g., steel cables. We will assume a nominal strain $\varepsilon = t/AE = 0.01$ in the cables of tensegrity A, and the 24 equivalent cables of tensegrity B (the additional cables in tensegrity B have a lower level of tension for equilibrium, and hence a lower nominal strain). In fact, a value of $\varepsilon = 0.01$ may be very large in these circumstances, and would correspond to a high tensile steel cable being stressed close to yield.

The results for the eigenvalues associated with Mode 1 and Mode 2 are presented in Table 1(a).

For Tensegrity A, Mode 1 is the most flexible mode (has the smallest eigenvalue), which reflects the fact that this is an infinitesimal mechanism, and to the first-order approximation of the stiffness matrix, there is no change in the length of any member for this mode. Thus the 'material' stiffness can contribute nothing to the stiffness, and the stiffness is entirely

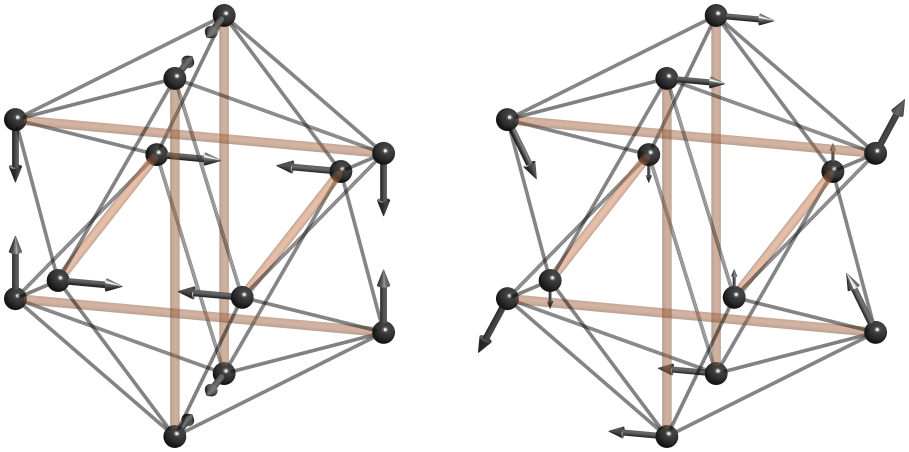

Mode 1 (a) Mode 2 (b)

Figure 4: The two modes considered in detail in Sections 3, 4 and 5. The modes are shown for Tensegrity A, but almost identical modes can be defined for Tensegrity B. (a) Mode 1 is the infinitesimal mechanism for Tensegrity A. (b) Mode 2 is a shear mode, with the structure shearing in the x-z plane; two other identical modes in the x-y and x-z planes exist.

generated from the reorientation of already stressed members. The stiffness of Mode 1 is proportional to the level of prestress in the structure, which will be clearly shown later in Figure 6(a.i).

For Tensegrity B, Mode 1 is not the most flexible mode. The additional cables added, when compared with tensegrity A, have ensured that Mode 1 is no longer an infinitesimal mechanism, and the stiffness of this mode is now far higher than the stiffness of the shear mode, Mode 2.

4 Compliant cables/high relative prestress

This section will consider the results that are appropriate for cases where the stiffness of the cables g is of a similar order to the value of the current tension coefficient t/l, for instance the case shown in Figure 3(b). This would be typical of tensegrities constructed with cables made of rubbers or other elastomers, or perhaps helically wound springs. Structures constructed in this way are unlikely to be used for civil engineering structures, but might be appropriate for highly compliant structures, e.g. tensegrity robots (Aldrich et al., 2003; Mirats Tur and Hernàndez Juan, 2009) or tensegrity springs (Azadi et al., 2009). Furthermore, demonstation models are often constructed with elastomeric cables (Pugh, 1976; Connelly and Back, 1998). We will assume a nominal strain $\varepsilon = t/AE = 0.6$ in the cables of Tenseg-

(a) Low prestress, $\varepsilon = 0.01$.

all $\times AE$	Tensegrity A	Tensegrity B
Mode 1	0.03	3.15
Mode 2	0.48	0.48

(b) High prestress, $\varepsilon = 0.6$.

all $\times AE$	Tensegrity A	Tensegrity B
Mode 1	1.96	4.97
Mode 2	0.34	0.40

Table 1: Eigenvalues of the stiffness matrix for two levels of prestress for the two tensegrities shown in Figure 1. Results are presented for the two modes shown in Figure 4.

rity A, and the 24 equivalent cables of Tensegrity B.

The results for the eigenvalues associated with Mode 1 and Mode 2 are presented in Table 1(b). For both Tensegrity A and Tensegrity B, the shear mode, Mode 2, is now the most flexible mode. Now the infinitesimal mechanism no longer dominates the behaviour of Tensegrity A, and the stiffness of this mode, Mode 1, is not as markedly different between Tensegrity A and Tensegrity B.

5 Zero-free-length cables

An extreme value of prestress is considered in this Section. When springs are wound helically, it is possible for them to be wound with pretension, where the coils of the spring are pressed against themselves when the spring is not loaded. For the correct level of pretension, the spring can be wound so that it has the tension/length properties shown in Figure 5: such springs are commonly used for static balancing, see, e.g., French and Widden (2000); Herder (2001).

If zero-free-length springs were used for either Tensegrity A or Tensegrity B, then the resultant structure has a zero stiffness mode. For this case, $\varepsilon = 1$ for all cables, and (neglecting the rigid struts) $\hat{\mathbf{G}} = \mathbf{0}$. Thus, in the formulation given in (6), the term $\mathbf{A}\hat{\mathbf{G}}\mathbf{A}^{\mathrm{T}}$ is zero, and only the stiffness resulting from the stress matrix $\mathbf{S}$ remains. However, this can provide no stiffness for shear modes, and thus Mode 2 has zero stiffness. Furthermore, the results of Schenk et al. (2007) show that this is not just a local phenomenon, and the structure could be deformed without limit, without any load being applied. In practice, of course, friction, and the limitations of the working length of the springs, will become important (Schenk et al., 2006).

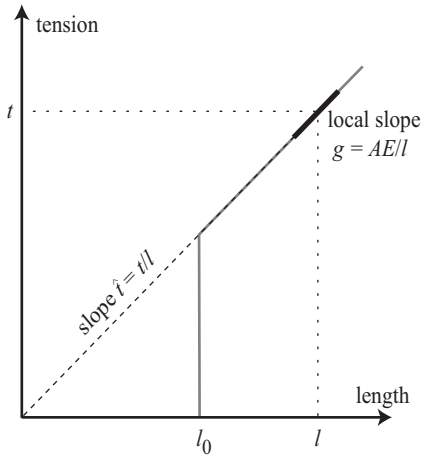

Figure 5: Material properties for a 'zero-free-length' spring. The spring is prestressed when coiled at length l_0. Initially, as tension is applied, this prestress is removed at approximately constant length. Then, within the working range, the spring has a tension proportional to its length, and hence $\hat{t} = t/l = dt/dl = g$.

Note that the existence of a zero stiffness shear mode for $\varepsilon = 1$ cannot be generalised to all tensegrities, as it depends critically on the orientation of the rigid struts. This is further discussed in Schenk et al. (2007).

6 Conclusion

Sections 3, 4 and 5 have shown how the dominant (softest) modes of Tensegrity A and Tensegrity B change as the relative level of prestress changes, described by the nominal strain ε. A complete overview of the stiffness changes is provided by the plots of the eigenvalues of the stiffness matrix for $0 \leq \varepsilon \leq 1$ given in Figure 6. In these plots, the eigenvalues have been normalised in two ways. In (a) the stiffness of the material remains constant, and ε is changed by varying the tension, t; however, to compare different materials, it may be more realistic to consider (b), where the tension t carried by the cables is held constant, and ε is changed by varying cable stiffness AE.

Figure 6 clearly shows that, for Tensegrity A, the most flexible mode for low values of ε is the infinitesimal mechanism shown as Mode 1, while for high values of ε the most flexible mode is the shear mode shown as Mode 2. In Tensegrity A, all cables are symmetrically equivalent, and so this example shows in a particularly clean way what we would expect to see for every tensegrity. For small values of ε, the key understanding of the

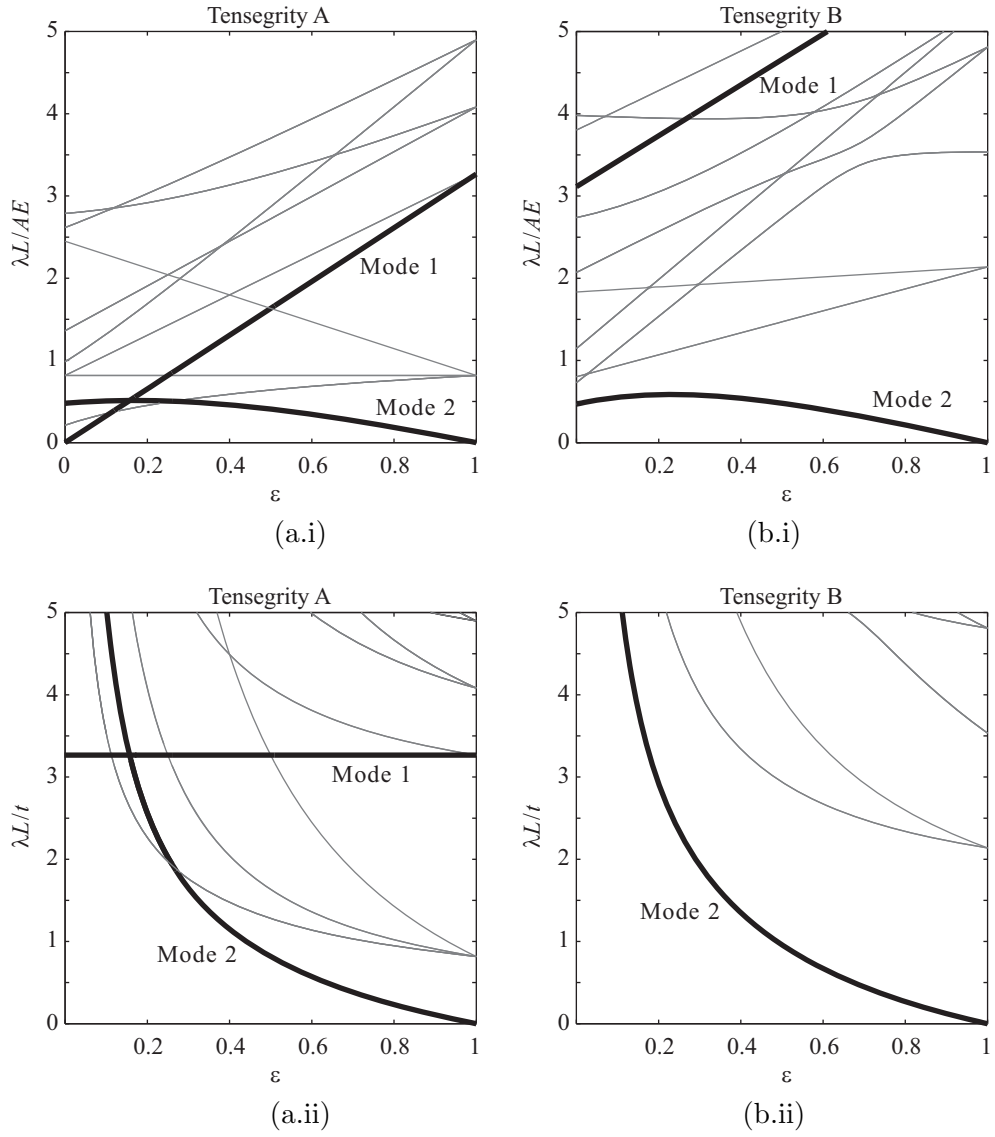

Figure 6: The complete set of eigenvalues λ of the stiffness matrix $\mathbf{K}$ for Tensegrity A (a.i and a.ii) and Tensegrity B (b.i and b.ii) for varying values of $\varepsilon = t/AE$. The eigenvalues for Mode 1 and Mode 2 are shown bold. For (a.i) and (b.i) the results are presented as $\lambda \times L/EA$, i.e., the stiffness of the cables is preserved as level of prestress varies. For (a.ii) and (b.ii) the results are presented as $\lambda \times L/EA \times 1/\varepsilon = \lambda \times L/t$, i.e., the tension in the cables is preserved as the cable stiffness varies. Assuming that the struts are rigid, and neglecting rigid-body modes, there are 24 eigenvalues in each plot, although symmetry ensures that there are at most only 10 distinct values.

structural behaviour comes about from understanding the equilibrium of the structure and the material properties, and hence the 'material' stiffness $\mathbf{AGA}^{\mathrm{T}}$, where $\mathbf{G} = \hat{\mathbf{G}}$ for $t = 0$. By contrast, for large values of ε, the understanding of the stiffness that comes from the stress matrix $\mathbf{S}$ is key, i.e., it is dominated by the stiffness that results from the reorientation of already stressed members.

If we were to extend the graphs in Figure 6 for $\varepsilon > 1$, we can see that both Tensegrity A and Tensegrity B would have a stiffness matrix with a negative eigenvalue, and hence even these super-stable tensegrities can be made unstable.

It should be noted that the results in Figure 6 are actually not valid for $\varepsilon = 0$, except for the zero value of the eigenvalue corresponding to Mode 1 for Tensegrity A. For any other mode of deformation, the calculation assumes some cables will go into compression, when in reality they would become slack. Different cables will go slack for different modes, and there is no longer a consistent tangent stiffness at this point. However, Roth and Whiteley (1981) show that all of these deformations will in fact have a positive stiffness.

Acknowledgements

I would like to thank R. Pandia Raj for his help with plotting the pictures of tensegrities.

References

Aldrich, J., Skelton, R., and Kreutz-Delgado, K. (2003). Control synthesis for a class of light and agile robotic tensegrity systems. In *Proceedings of the American Control Conference, Denver, Colorado, June 4–6 2003*.

Altmann, S. L. and Herzig, P. (1994). *Point-Group Theory Tables*. Clarendon Press, Oxford.

Azadi, M., Behzadipour, S., and Faulkner, G. (2009). Antagonistic variable stiffness elements. *Mechanism and Machine Theory*, 44(9):1746–1758.

Calladine, C. R. (1978). Buckminster Fuller's "Tensegrity" structures and Clerk Maxwell's rules for the construction of stiff frames. *International Journal of Solids and Structures*, 14:161–172.

Cauchy, A. L. (1813). Recherche sur les polyèdres — premier mémoire. *Journal de l'École Polytechnique*, 9:66–86.

Connelly, R. (1999). Tensegrity structures: why are they stable? In Thorpe, M. F. and Duxbury, P. M., editors, *Rigidity Theory and Applications*, pages 47–54. Kluwer Academic/Plenum Publishers.

Connelly, R. and Back, W. (1998). Mathematics and tensegrity. *American Scientist*, 86:142–151.

Connelly, R. and Whiteley, W. J. (1996). Second-order rigidity and prestress stability for tensegrity frameworks. *SIAM Journal of Discrete Mathematics*, 7(3):453–491.

Dehn, M. (1916). Über die starreit konvexer polyeder. *Mathematische Annalen*, 77:466–473.

French, M. J. and Widden, M. B. (2000). The spring-and-lever balancing mechanism, George Carwardine and the Anglepoise lamp. *Proceedings of the Institution of Mechanical Engineers part C – Journal of Mechanical Engineering Science*, 214(3):501–508.

Guest, S. D. (2006). The stiffness of prestressed frameworks: a unifying approach. *International Journal of Solids and Structures*, 43:842–854.

Heartney, E. (2009). *Kenneth Snelson: Forces Made Visible*. Hudson Hills Press LLC.

Herder, J. L. (2001). *Energy-Free Systems. Theory, Conception and Design of Statically Balanced Spring Mechanisms*. PhD thesis, Delft University of Technology.

Kangwai, R. D. and Guest, S. D. (2000). Symmetry-adapted equilibrium matrices. *International Journal of Solids and Structures*, 37:1525–1548.

Kangwai, R. D., Guest, S. D., and Pellegrino, S. (1999). An introduction to the analysis of symmetric structures. *Computers and Structures*, 71:671–688.

Masic, M., Skelton, R. E., and Gill, P. E. (2006). Optimization of tensegrity structures. *International Journal of Solids and Structures*, 43(16):4687–4703.

Mirats Tur, J. M. and Hernàndez Juan, S. (2009). Tensegrity frameworks: Dynamic analysis review and open problems. *Mechanism and Machine Theory*, 44(1):1–18.

Motro, R. (2003). *Tensegrity Structural Systems for the Future*. Kogan Page Science.

Pellegrino, S. (1993). Structural computations with the singular value decomposition of the equilibrium matrix. *International Journal of Solids and Structures*, 30(21):3025–3035.

Pellegrino, S. and Calladine, C. R. (1986). Matrix analysis of statically and kinematically indeterminate frameworks. *International Journal of Solids and Structures*, 22:409–228.

Pugh, A. (1976). *Introduction to Tensegrity*. University of California Press., Berkeley.

Roth, B. and Whiteley, W. (1981). Tensegrity frameworks. *American Mathematical Society*, 265(2):419–446.

Schenk, M., Guest, S. D., and Herder, J. L. (2007). Zero stiffness tensegrity structures. *International Journal of Solids and Structures*, 44:6569–6583.

Schenk, M., Herder, J. L., and Guest, S. D. (2006). Design of a statically balanced tensegrity mechanism. In *Proceedings of DETC/CIE 2006, ASME 2006 International Design Engineering Technical Conferences & Computers and Information in Engineering Conference September 10-13, 2006, Philadelphia, Pennsylvania, USA*.

Skelton, R. and de Oliveira, M. (2009). *Tensegrity Systems*. Springer.